Alcohol-Induced Change of ''Reverse Osmosis'' Polyamide Membrane Surface

Vinod K. Agrawal,[1] Puyam S. Singh[2]

[1]*Analytical Science Division, Central Salt and Marine Chemicals Research Institute (Council of Scientific and Industrial Research), G.B. Marg, Bhavnagar 364002, Gujarat, India*
[2]*RO Membrane Division, Central Salt and Marine Chemicals Research Institute (Council of Scientific and Industrial Research), G.B. Marg, Bhavnagar 364002, Gujarat, India*

Received 17 February 2011; accepted 25 November 2011
DOI 10.1002/app.36561
Published online 26 January 2012 in Wiley Online Library (wileyonlinelibrary.com).

ABSTRACT: An analysis method based on Attenuated total reflectance infra-red spectroscopy was used to measure water and alcohol sorption from water–methanol and water–isopropanol aqueous solutions in the ''reverse osmosis" polyamide membrane. Preferential sorption of water over alcohol was observed in the membrane. As alcohol concentration in the solution increases, the sorption selectivity of water over methanol increases from 4 to 375, whereas the sorption selectivity water over isopropanol increases only from 2 to 8. However, as water is nonsolvent for polyamide, the membrane surface structure remains unaffected by the water sorption. On the other hand, the sorption of alcohol in the membrane leads to decrease in characteristic IR band intensities of the polyamide implying a change in membrane surface structure which corroborates with the change in membrane surface roughness as observed by atomic force microscopy (AFM) and scanning electron microscopy (SEM) images. © 2012 Wiley Periodicals, Inc. J Appl Polym Sci 124: E290–E299, 2012

Key words: infrared spectroscopy; polyamide; membrane; surfaces; morphology

INTRODUCTION

The reverse osmosis (RO) polyamide membrane[1]is a thin-film-composite membrane comprised top ultrathin skin polyamide layer, middle polysulfone porous support, and bottom nonwoven fabric. The top polyamide layer is active barrier layer which is a crosslinked polyamide network formed by interfacial polymerization of *m*-phenylenediamine monomer dissolved in water and trimesoylchloride monomer dissolved in organic solution and is mainly responsible for permeability and selectivity. The RO polyamide membrane is widely used for water desalination, water reclamation, and waste water treatments.[2–4] However, the RO membranes lack resistance in most of the organic solvents; therefore, the application of RO polyamide membrane in the separation of organics is very limited. The stability of the membrane in the organic solvent is dependent on the nature of interaction between the organic molecules and polymer chains. The membrane structure may be altered due to the change in polymer nanostructure caused by interaction between the polymer chains and organics. These interactions can be related to the solubility parameters of the polymer and solvent. When exposure to solvent of similar solubility parameter occurs, dissolution of linear polymers of small molecular weights or swelling of crosslinked polymers will be resulted.[5] The swelling of polymer can be extreme and sometimes plasticization of polymer might occur when the solubility parameter difference between the polymer and solvent is small. With large differences between the polymer and solvent solubility parameters, the solvent will have no immediate effect but some swelling of polymer may still occur after a prolong exposure to the polymer to such solvents. The change in performance of RO polyamide membrane on chemical or solvent treatment has been reported.[6,7] A strong interaction between polyamide and isopropanol has been observed due to the closeness of their solubility parameter values.[8–10] This may cause a change in membrane properties as a result of polymer chain movement as the membrane porosity arises from the spaces between the segments constituting the polymer network within each supramolecular polymer aggregate as well as the spaces between neighboring supramolecular polymer aggregates themselves.[11–13] The pores of the polyamide membranes are of noninterconnecting type.[14,15] The size of polymer aggregates was measured as about 10–20 nm in diameter and highly compacted but can be loosened by solvent treatment.[16] Further, the polymer chain nanostructure can be modified by the introduction of nanoparticles resulting to a change in membrane pore size.[17,18] Therefore, it is important to understand that how the interaction of alcohol to the polymer

Correspondence to: P. S. Singh (puyam@csmcri.org).

chain network affects the morphology of supramolecular polymer aggregate consequently to the change of the RO polyamide membrane performance and life-time. Methanol and isopropanol are the primary and secondary alcohol, respectively. The difference of solubility parameter value between the polyamide membrane material and methanol is higher than the difference of solubility parameter value between the polyamide and isopropanol signifying relatively a higher degree of interaction of isopropanol with the polyamide material. Therefore, it is interesting to study the extent of changes on the polymeric membrane surface and properties by the different degree of interaction between the polymer and alcohol.

Attenuated total reflectance infra-red (ATR-IR) spectroscopy[19–21] and atomic force microscopic techniques[22–24] are suitable techniques to study the surfaces of the RO polyamide membranes. These techniques are nondestructive techniques which can measure the samples in their native forms and therefore particularly suited to study the alcohol sorption in the membrane. Based on ATR-IR spectroscopy, we used an analysis method to measure water and alcohol sorption from water–methanol and water–isopropanol aqueous solutions in the RO polyamide membrane. The characteristic IR peaks of the polyamide chains before and after the alcohol sorption were examined and correlated with the change in surface topology observed by atomic force microscopy images. Scanning electron microscopy images of neat and treated membrane samples were also measured to check the change in surface microstructure of membrane before and after the alcohol sorption.

EXPERIMENTAL

Materials

Methanol (99.8%) and isopropanol (99.8%) were obtained from SRL, India. RO polyamide membranes were prepared by interfacial polymerization based on a reported procedure.[19] Sorption experiments were performed by contacting the membrane with aqueous solutions of different concentrations of alcohol in a range from 0 to 99% (v/v). The contact time is for 2 h to make ensure equilibrium sorption of the alcohols in the membrane. The equilibrium sorption time was fixed based on the sorption uptake of the alcohol in the sample with time.

ATR-IR spectral analysis

The ATR-IR instrument used consisted of a Barnes model 300 continuously variable ATR accessory interfaced to a Nicolet 5DX Fourier transform infrared spectrometer. Thirty-two scans were performed for each sample with scan velocity of 0.2 cm s^{-1} and sampling time of 160 s to provide good statistical measurements of absorbance peaks of functional groups present. The germanium crystal was fixed at 45°C angle of incidence, which gave a probing depth of submicrometer range of 0.17–0.69 μm corresponding to 1000–4000 cm^{-1} in the chemical infrared region of interest. The membrane samples were mounted on both faces of germanium crystal, the active layer facing the crystal surface. Depth of penetration of the beam into the sample varies proportionately with wavelength (λ). Using the value of penetration depth and IR absorbance peak intensity, the film thickness can be approximately calculated as reported elsewhere.[19,21] ATR-IR of aqueous alcohol solutions were performed by spreading solution on the faces of germanium crystal. The measurements for each sample were repeated at least five times to get a reliable data. The intensities of the spectra was found to be nearly the same for each measurement indicating no appreciable loss of alcohol due to evaporation occurred during the each scan of 5 s.

The sorption selectivity of water over alcohol in the membrane was estimated using the following expression.

$$\alpha_{w/a} = \frac{[C_w/C_a]_{\text{membrane}}}{[C_w/C_a]_{\text{solution}}} \quad (1)$$

where C_w and C_a are the concentration of water in the membrane and in solution, respectively.

AFM images analysis

Surface topologies of the flat sheet membranes were observed using and atomic force microscopy (NT-MDT instrument, a product of NT-MDT Co. Building 100, Zelenograd, Moscow 124482, Russia). The AFM image scans in four different locations of membranes were performed to get a reliable data for a representative AFM surface image observation of each membrane sample. The following statistical characteristics for the flat sheet membrane surfaces were estimated by roughness analysis of the AFM surface images. $Z_{ij} = Z(X_i,Y_j)$ is the source discrete function defined in the XY-plane; N_x and N_y are X and Y dimensions. The mean value of peak-to-peak distance, the first moment of the distribution, is expressed as

$$\mu = \frac{1}{N_x.N_y}\sum_{j=1}^{N_y}\sum_{i=1}^{N_x} Z_{ij} \quad (2)$$

The average arithmetic roughness (average roughness) as

$$S_a = \frac{1}{N_x.N_y}\sum_{j=1}^{N_y}\sum_{i=1}^{N_x} \left|Z_{ij} - \mu\right| \quad (3)$$

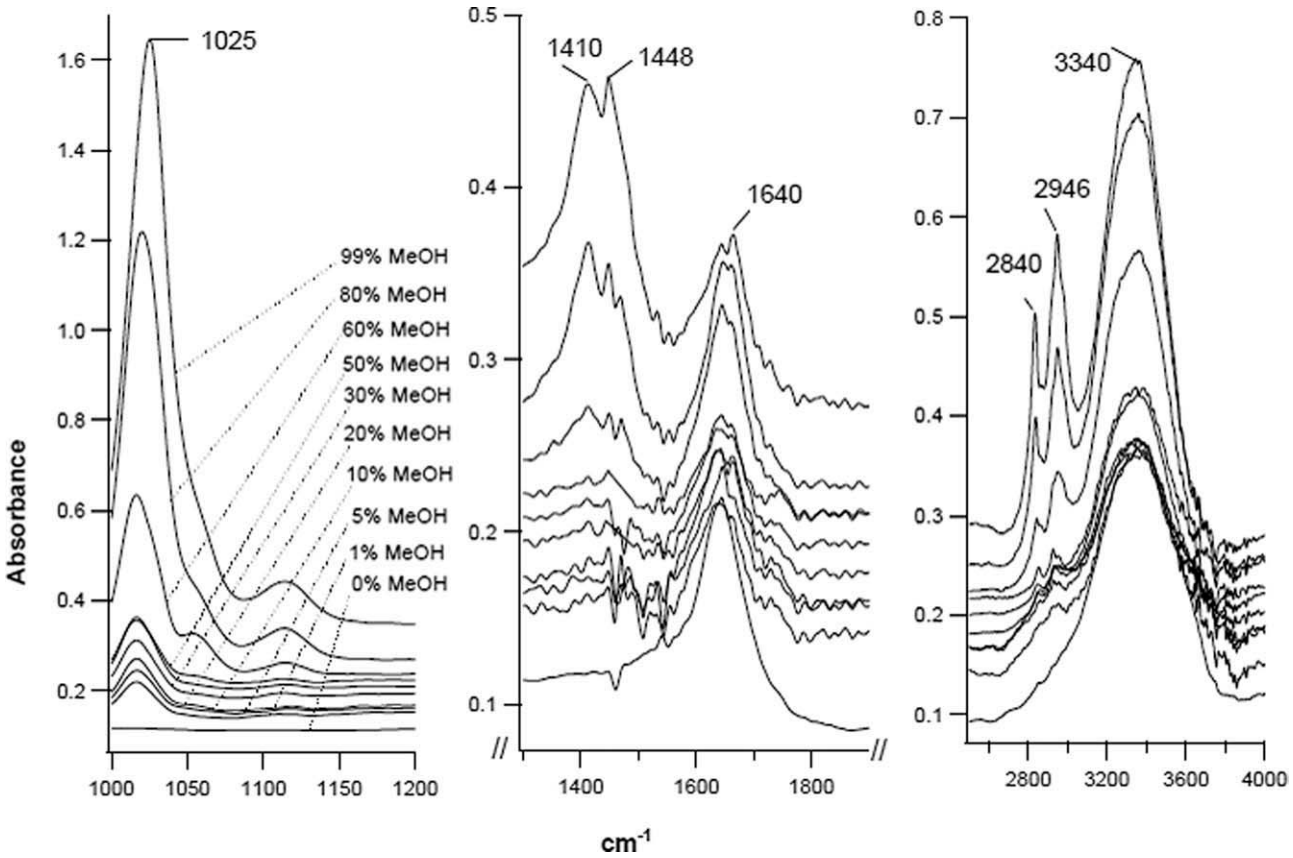

Figure 1 IR-spectra of water-methanol solutions with methanol concentration in a range of 0–99 vol %.

The root mean square roughness as

$$S_q = \sqrt{\frac{1}{N_x.N_y}\sum_{j=1}^{N_y}\sum_{i=1}^{N_x}\left(Z_{ij}-\mu\right)^2} \qquad (4)$$

SEM pictures of the samples were taken on LEO 1430VP scanning electron microscope. The samples are sputter coated with gold before SEM observation. The coating was tuned to obtain optimum grain size and noncontinuous coating as to not have an effect on the surface morphology of the samples.

RESULTS AND DISCUSSION

ATR-IR spectral analysis of aqueous alcohol solutions

The IR-spectra of water–methanol solutions with methanol concentration in a range of 0–99% (v/v) are shown in Figure 1. The IR peak intensities of the solution mixtures at 2946, 2840, 1448, 1410, and 1025 cm^{-1} increase, whereas the peak intensity at 1640 cm^{-1} decreases with increase in methanol concentration. The area and height of peak at 2946 and 2840 cm^{-1} characteristic of aliphatic stretching vibration was used to estimate the methanol amount, whereas the peak at 1640 cm^{-1} characteristic of water bending mode vibration was used to estimate the amount of water. Both the peak areas and heights of absorbance peaks were used for calculation. The percent IR methanol peak intensities was calculated as $100 \times [I_{2840-2946}/(I_{1640} + I_{2840-2946})]$, and the percent IR water peak intensities was calculated as $100 \times [I_{1640}/(I_{1640} + I_{2840-2946})]$. Figure 2 shows a plot of "as-prepared" methanol–water composition against the percent IR methanol peak intensities. As seen from the plot, there is a "nearly linear" relationship between the actual compositional ratios and the percent IR peak intensities. It can further be noticed from the plot that the IR response of water is almost double of the IR response of methanol. Nevertheless, an increase in the IR intensities as a function of material amount was clearly observed in the plot. It was, therefore, possible to calculate the percentage of alcohol for a given aqueous alcohol solution by measuring the IR peak intensities and using the correlation between the IR peak intensities and the solution concentration. Similar result of linear relationship between the actual compositional ratios and the percent IR peak intensities was found for the isopropanol–water solution mixtures. Selected IR spectra of the isopropanol–water solutions are shown in Figure 3. The bands 2974, 2877, 1466, 1307, 1160, and

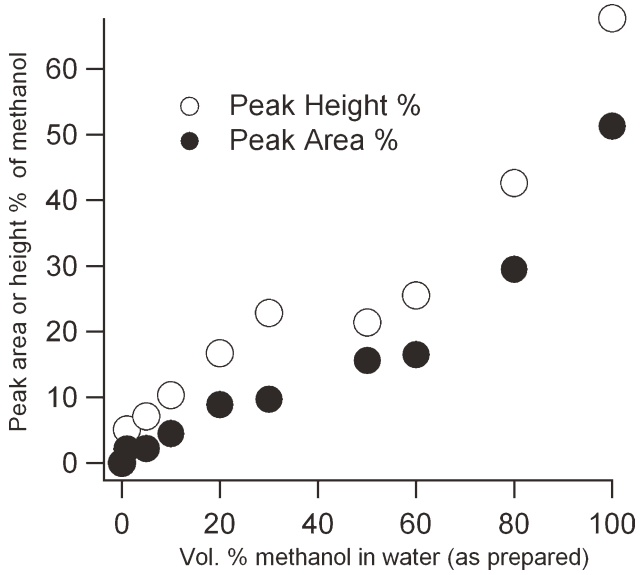

Figure 2 A plot of "as-prepared" methanol–water composition against the IR peak area and height % of methanol (2840–2946 cm^{-1}) band; The percent IR peak intensities are calculated as $100 \times [I_{2840-2946}/(I_{1640} + I_{2840-2946})]$. The peak at 1640 cm^{-1} and 2840–2946 cm^{-1} corresponding of water and aliphatic stretching vibration, respectively, are considered for the calculation.

1130 cm^{-1} corresponds to absorbance peaks of isopropanol. These band intensities were found to increase with increase in isopropanol concentration in the aqueous solution which is a similar case with the spectra of water–methanol solutions.

Absorption of aqueous methanol solutions in the RO polyamide membrane

Figure 4 shows ATR-IR spectra of the RO polyamide membranes after absorbed with water–methanol aqueous solutions. MS1, MS2, MS3, MS4, MS5, MS6, MS7, MS8, MS9, and MS10 corresponds to membrane samples absorbed with aqueous solutions of 0, 1, 5, 10, 20, 30, 50, 60, 80, and 99% (v/v) methanol in water, respectively. Only weak absorption of methanol in the membrane surface was apparent as evident from weak absorbance peaks at 2946 and 2840

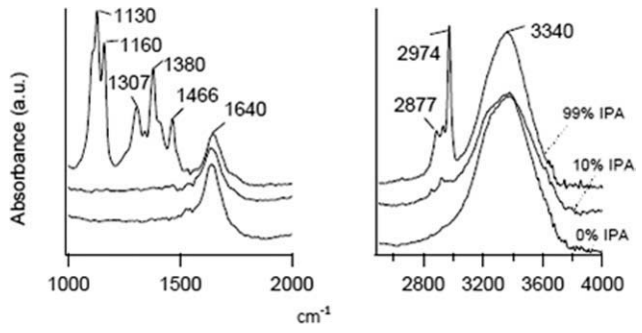

Figure 3 IR spectra of the isopropanol–water solutions.

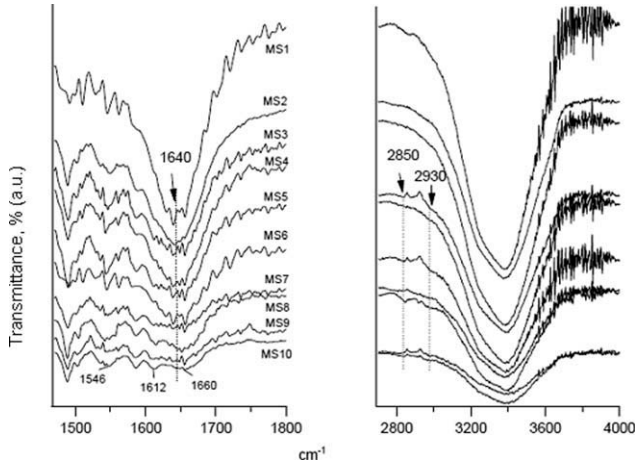

Figure 4 ATR-IR spectra of the RO polyamide membranes after absorbed with water–methanol aqueous solutions.

cm^{-1} characteristic of aliphatic stretching vibration modes for the samples absorbed with the aqueous solutions of 10–99% methanol concentration. Strong absorbance peak at 1640 cm^{-1} due to bending vibration mode of water was observed in the samples absorbed with aqueous solution of 0–10% methanol concentration. In such samples absorbed with a large amount of water, the characteristic polyamide peaks of 1546 (amide II, C=N stretch), 1612 (aromatic ring breathing), 1660 cm^{-1} (amide I, C=O stretch), were buried in the strong absorbance peak of water which, however, clearly were seen in the samples absorbed with a smaller amount of water from aqueous solution of high alcohol content. This can be explained on the basis that the membrane surface is fully covered with water layer for the sample absorbed with a larger amount of water; thickness of the water layer is in a length-scale well beyond the ATR-IR penetration depth of submicrometer range. The IR spectra of water obtained by subtracting the base peaks of polyamide are shown in Figure 5. The decrease in the intensities of the absorbance peaks at 1640 and 3340 cm^{-1} were observed for the sample series after absorption with aqueous solutions containing increasing amount of methanol concentration. The % water sorption uptake is on the basis of (weight of water)/(weight of water and polymer), whereas the % methanol sorption uptake is on the basis of (weight of methanol)/(weight of methanol and polymer). The height of absorbance peak at 1640 cm^{-1} was considered to estimate approximate amount of water sorption with reference to the absorbance peak height measured as 0.132 obtained from ATR-IR spectrum of 100% water. On the other hand, the height of absorbance peak at 2946 cm^{-1} was considered to estimate amount of methanol with reference to the absorbance peak height measured as 0.175 obtained from ATR-IR spectrum of

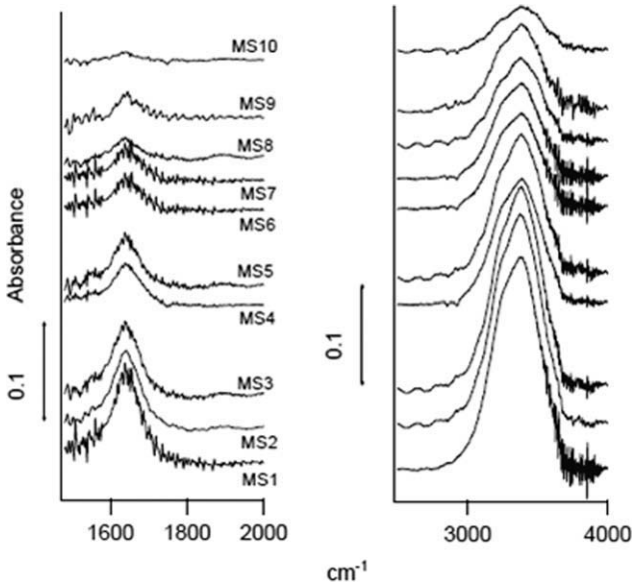

Figure 5 The IR spectra of absorbed water.

100% methanol. The calculated water and methanol sorption uptake percentages are given in Table I. The water sorption uptake in the membrane increases (up to 70%) with increasing water content in the water–methanol solution, whereas the methanol sorption uptake remains nearly constant at about 1%. This means the sorption of methanol in the polymer material is limited as expected from the large difference between the solubility parameter of methanol and polyamide. According to Hoftyzer and Van Krevalen method, the solubility parameter of aromatic polyamide[25] is predicted as 7.9, whereas the solubility parameter of methanol is 14.5. Using the sorption uptake values and eq. (1), the water sorption selectivity factor ($\alpha_{w/a}$) are calculated. The $\alpha_{w/a}$ values range from 4 to 375 indicating preferential sorption of water over methanol.

Absorption of aqueous isopropanol solutions in the RO polyamide membrane

Figure 6 shows ATR-IR spectra of the RO polyamide membranes after absorbed with water–isopropanol aqueous solutions. IPS1, IPS2, IPS3, IPS4, IPS5, IPS6, IPS7, IPS8, IPS9, and IPS10 corresponds to membrane samples absorbed with aqueous solutions of 0, 1, 5, 10, 20, 30, 50, 60, 80, and 99% isopropanol in water, respectively. Absorption of isopropanol in the membrane surface was apparent as evident from absorbance peaks at 2974 cm^{-1} characteristic of aliphatic stretching vibration modes for the samples absorbed with the aqueous solutions of 1–99% isopropanol concentration. The decrease and increase in the intensities of the absorbance peaks at 1640 and 2974 cm^{-1}, respectively, were observed for the sample series after absorption with aqueous solutions containing increasing amount of isopropanol concentration. As done above in case of water–methanol sorption, the height of absorbance peak at 1640 cm^{-1} was considered to estimate amount of water sorption, whereas the height of absorbance peak at 2974 cm^{-1} was considered to estimate amount of isopropanol. The absorbance peak height at 2974 cm^{-1} band was measured as 0.175 in the ATR-IR spectrum for 100% isopropanol which is exactly similar height as that of 100% methanol peak. The calculated water and isopropanol sorption uptake percentages are given in Table II. The isopropanol sorption uptake in the membrane increases (up to 50%) with increasing isopropanol content in the aqueous solution while the water sorption uptake remains nearly similar as in the case of water–methanol solutions. The strong sorption of isopropanol in the polymer material is expected as the solubility parameter of isopropanol is 8.8, which is close to the solubility parameter value of the aromatic polyamide. Using the sorption uptake values and eq. (1), the water

TABLE I
The Percentages of Water and Methanol Sorption Uptake and Corresponding Water Sorption Selectivity

Samples	Absorbance peak height of 1640 cm^{-1}	Water sorption uptake (%)	Absorbance peak height of 2946 cm^{-1}	Methanol % in aqueous solution	Water sorption selectivity ($\alpha_{w/a}$)
MS1	0.092	70	0	0	–
MS2	0.080	61	0	1	–
MS3	0.073	55	0	5	–
MS4	0.044	33	Trace[a]	10	4
MS5	0.044	33	Trace	20	8
MS6	0.032	24	Trace	30	10
MS7	0.031	23	Trace	50	23
MS8	0.020	15	Trace	60	23
MS9	0.019	14	Trace	80	57
MS10	0.005	4	Trace	99	375

[a] Trace = estimated about 0.001–0.002 absorbance corresponding to ~ 1% methanol sorption uptake for the samples MS4–MS10.

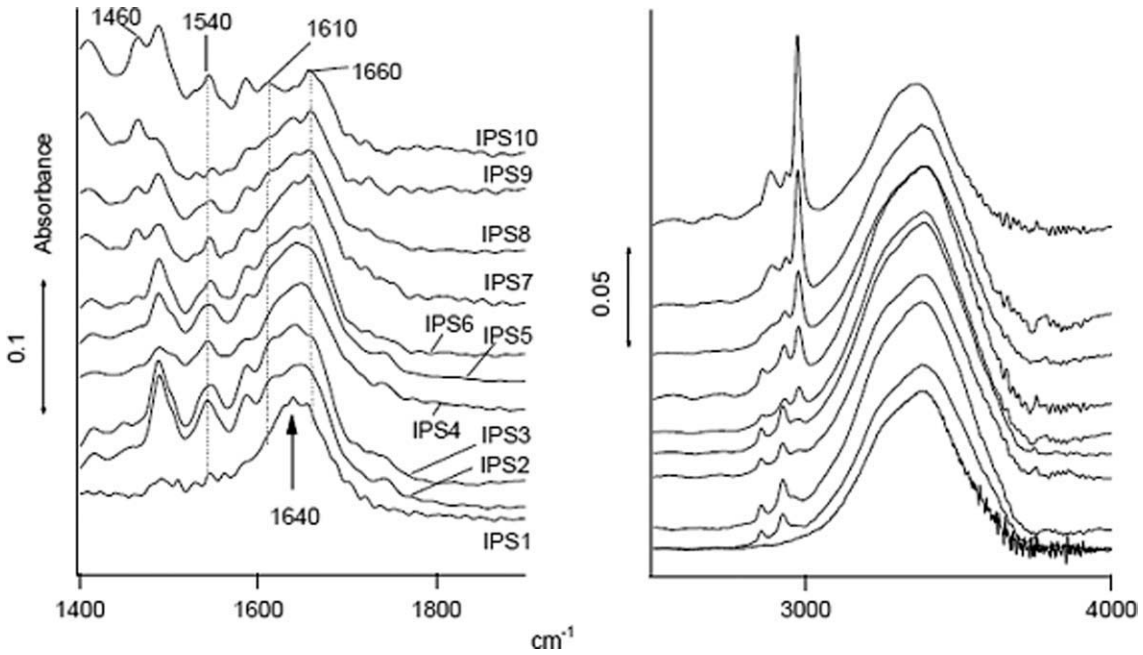

Figure 6 ATR-IR spectra of the RO polyamide membranes after absorbed with water–isopropanol aqueous solutions.

sorption selectivity factor ($\alpha_{w/a}$) is calculated. The maximum $\alpha_{w/a}$ values obtained was about 8 only in this case which is about 47 times decrease from the maximum $\alpha_{w/a}$ value of 375 obtained in case of water–methanol solutions. This implies stronger absorption of isopropanol than methanol in the membrane.

Change in the polyamide structure after absorption with alcohol as observed by ATR-IR

The membranes after absorption with aqueous alcohol solutions were dried at room temperature for 24 h to remove the absorbed liquids from the membrane surfaces. The surface chemical structures of the dry membranes were then examined by ATR-IR. Figures 7 and 8 show ATR-IR spectra for the series of dry membranes obtained from water–methanol and water–isopropanol treatments, respectively. In both, the cases of aqueous methanol and aqueous isopropanol-treated samples, there is a decreasing trend in the 1660 cm^{-1} absorbance peak which is characteristic peak of C=O amide of polyamide chain networks. Table III shows the values of the 1660 cm^{-1} absorbance peak and relative changes in the peak intensity and area after the treatments of the samples with aqueous methanol and isopropanol solutions. The 1660 cm^{-1} peak intensity decreases to about half of the original intensity for the sample treated with 99% methanol or 99% isopropanol. If there is no change in the membrane surface topology, the decrease in the absorbance peak intensity at 1660 cm^{-1} shall imply a decrease in polyamide layer thicknesses based on the relationship between the layer thickness, IR intensity, and IR penetration depth. However, the peak intensity cannot be simply

TABLE II
The Percentages of Water and Isopropanol Sorption Uptake and Corresponding Water Sorption Selectivity

Samples	Absorbance peak height of 1640 cm^{-1}	Water sorption uptake (%)	Absorbance peak height of 2974 cm^{-1}	Isopropanol sorption uptake (%)	Isopropanol % in aqueous solution	Water sorption selectivity ($\alpha_{w/a}$)
IPS1	0.091	69	0		0	–
IPS2	0.089	68	0.001	0.3	1	2
IPS3	0.085	64	0.002	0.9	5	4
IPS4	0.069	52	0.003	1.7	10	3
IPS5	0.071	54	0.006	3.4	20	4
IPS6	0.062	47	0.008	4.6	30	4
IPS7	0.055	41	0.019	10.9	50	4
IPS8	0.048	36	0.028	15.8	60	3
IPS9	0.035	27	0.058	33.2	80	3
IPS10	0.005	4	0.087	49.5	99	8

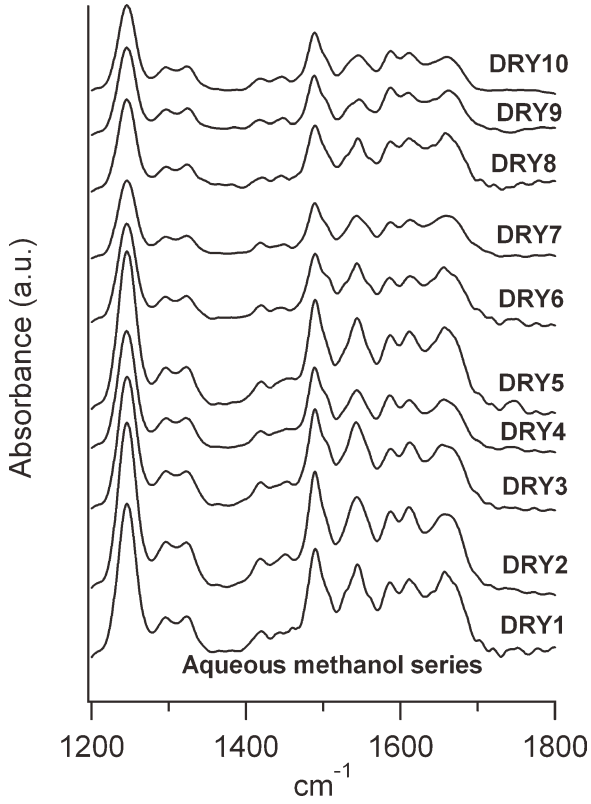

Figure 7 ATR-IR spectra for the series of dry membranes obtained after the treatment with aqueous methanol solutions.

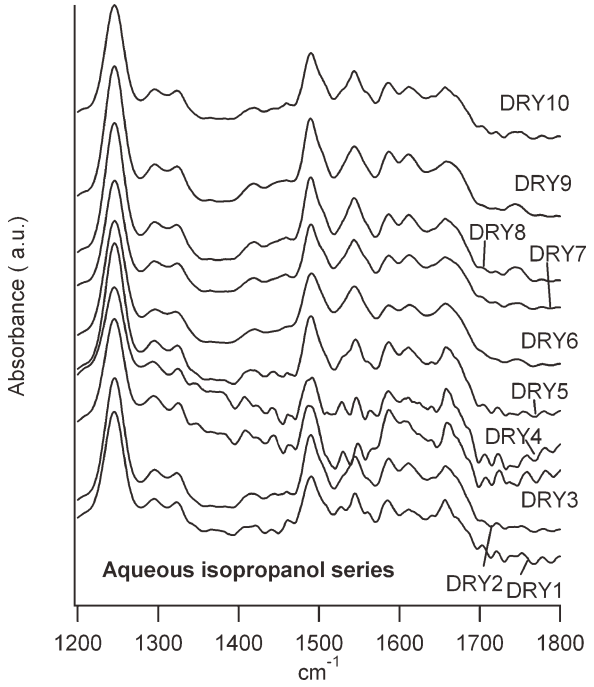

Figure 8 ATR-IR spectra for the series of dry membranes obtained after the treatment with aqueous isopropanol solutions.

related with the layer thickness if there is a change in surface topology. In the case where there is a change in surface roughness before and after the alcohol solution treatments, the ATR-IR of a fixed penetration depth shall encounter a difference in materials density of the samples relative to their surface heterogeneities. As it is understood that the RO polyamide does not dissolve in alcohol, one can expect nonremoval of the polyamide layer on the alcohol solution treatment. Therefore, the observed change in the polyamide intensity may be related to a change in surface topology as the IR penetration depth (0.17–0.69 μm) is in the range of surface roughness values of the "reverse osmosis" polyamide membrane surfaces. Furthermore, in the case of aqueous methanol sample series, all the other peaks in addition to 1660 cm^{-1} band also show a decreasing trend. This can be explained based on large solubility parameter difference between the polyamide material and methanol, whereas there is closeness of

TABLE III
Absorbance Peak Heights and Areas of 1660 cm^{-1} IR Band for the Dry Samples after the Treatments with Aqueous Alcohol Solutions

Samples	% Alcohol in aqueous solution	Aqueous methanol series				Aqueous isopropanol series			
		Height[a]		Area[a]		Height[a]		Area[a]	
		Abs.	%	Abs.	%	Abs.	%	Abs.	%
DRY1	0	0.031	100	1.690	100	0.031	100	1.690	100
DRY2	1	0.028	89	1.529	90	0.024	76	1.099	65
DRY3	5	0.024	77	1.348	80	0.024	77	0.682	40
DRY4	10	0.020	63	1.052	62	0.024	78	0.891	53
DRY5	20	0.020	62	1.069	63	0.025	79	1.018	60
DRY6	30	0.017	55	1.000	59	0.024	77	1.135	67
DRY7	50	0.016	52	0.646	38	0.018	59	0.897	53
DRY8	60	0.016	52	0.945	56	0.021	67	0.961	57
DRY9	80	0.015	48	0.806	48	0.019	62	0.875	52
DRY10	99	0.015	47	0.759	45	0.018	59	0.881	52

[a] Percent change is calculated with reference to the absorbance values of the dry sample which was treated with pure water; the value of 100 was taken for this sample.

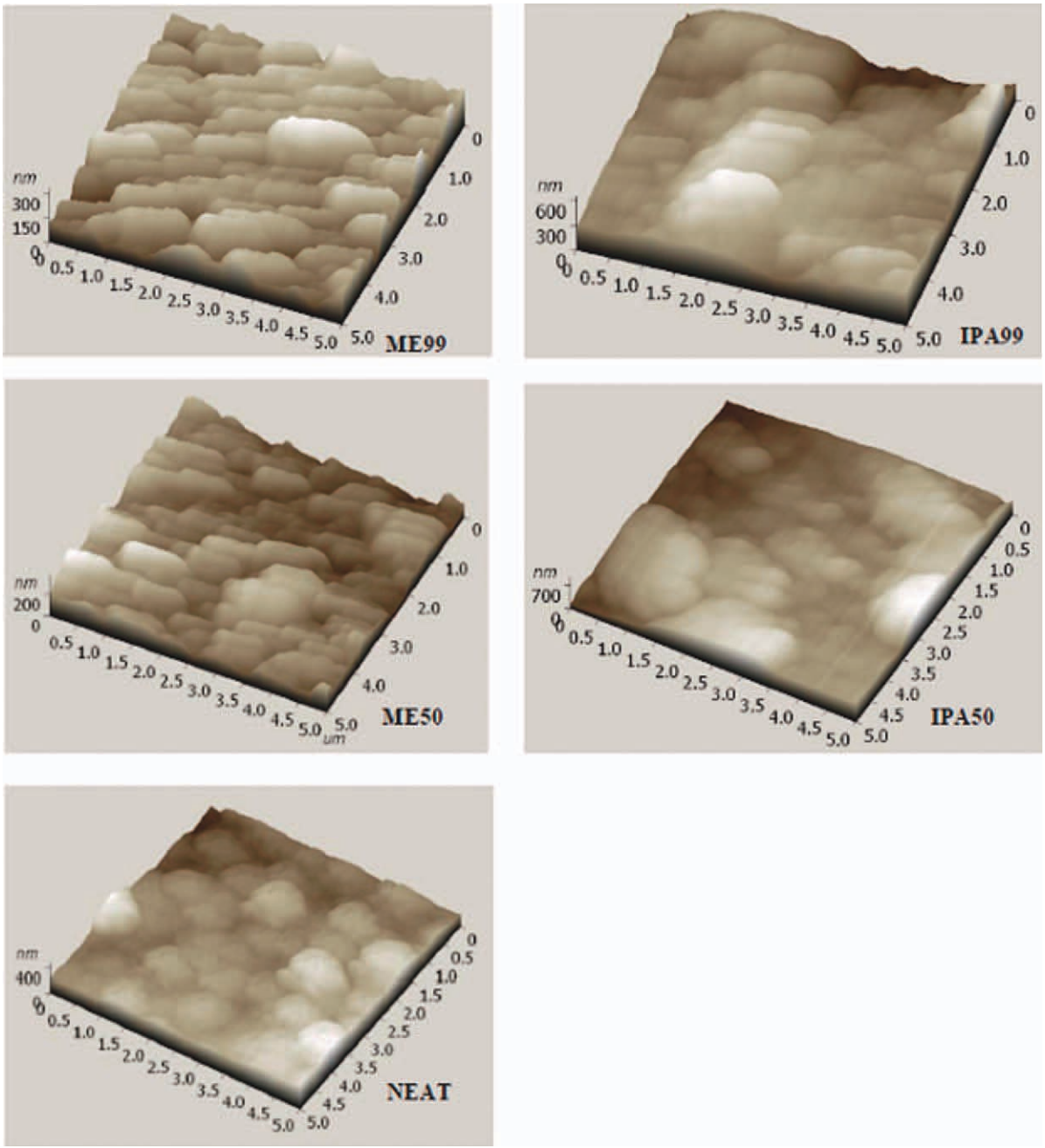

Figure 9 AFM images of the neat and the alcohol solution-treated samples in 5×5 μm^2 image size. [Color figure can be viewed in the online issue, which is available at wileyonlinelibrary.com.]

solubility parameter between the polyamide material and isopropanol. As a result, there is stronger interaction of isopropanol with the polyamide material leading to change in aggregated polymer chain networks, subsequently to the major change of intensity of polyamide functional group. On the other hand, only weak interaction of methanol with the polymer chains may occur as the methanol sorption in the polymer materials is very low; therefore, the overall change in intensities of the peaks of aqueous methanol samples series may be related to the changes in surface roughness of the membranes. To verify the hypothesis, the AFM images were taken on the samples before and after the alcohol solutions treatments.

AFM study of the membrane surface before and after the alcohol treatments

AFM study was performed on the membrane samples to examine the surface topology of the samples before and after the aqueous solution treatments. The treatment was performed by immersing the

TABLE IV
The Peak-to-Peak Maximum Distance (S_y), the Mean Value of Peak-to-Peak Distance (the First Moment of Distribution) (μ), the Average Arithmetic Roughness (S_a), and the Root Mean Square Roughness (S_q) for the Membrane Samples

Samples	S_y (μm)	μ (μm)	S_a (μm)	S_q (μm)
Analysis of 5 × 5 μm^2 image frame				
NEAT	0.499	0.262	0.064	0.081
ME50	0.936	0.449	0.183	0.215
ME99	0.984	0.483	0.146	0.182
IPA50	1.169	0.547	0.215	0.260
IPA99	0.967	0.425	0.185	0.217
Analysis of 20 × 20 μm^2 image frame				
NEAT	0.926	0.430	0.124	0.157
ME50	1.667	0.929	0.285	0.351
ME99	1.713	0.636	0.259	0.317
IPA50	1.804	0.703	0.320	0.374
IPA99	2.132	0.934	0.350	0.425

ME50 and ME99 are the samples after treatment with aqueous alcohol solutions of 50 and 99% methanol, respectively; IPA50 and IPA99 are the samples after treatment with aqueous alcohol solutions of 50 and 99% isopropanol, respectively; NEAT is the sample without the treatment.

membrane film in the aqueous alcohol solutions for 2 h followed by drying at room temperature for 5 h. ME50 and ME99 are the samples after treatment with aqueous alcohol solutions of 50 and 99% methanol, respectively, whereas IPA50 and IPA99 are the samples after treatment with aqueous alcohol solutions of 50 and 99% isopropanol, respectively. NEAT (fresh RO membrane) is the sample without the treatment. Figure 9 shows the AFM images of the samples in 5 × 5 μm^2 image size. As shown in Figure 9, the surface morphology of the NEAT sample shows a typical nodular morphology of reverse osmosis polyamide membrane,[24] and each nodular unit is comprised of nanoscale compacted blocks similar to the small-angle neutron scattering results reported elsewhere.[16] The surface topologies of the membranes on the aqueous alcohol treatments are shown to differ as revealed in the AFM images. The size of nodular units have been changed to a larger value, and second, the nanoscale compacted blocks of the nodular units are no longer visible in the samples after the aqueous alcohol solution treatments. The peak-to-peak maximum distance (S_y), the mean value of peak-to-peak distance (the first moment of distribution) (μ), the average arithmetic roughness (S_a), the root mean square roughness (S_q) for the membrane samples are given in Table IV. It can be noted that the surface roughness parameter values differ between the projection areas of 20 × 20 μm^2 and 5 × 5 μm^2 image sizes. Therefore, comparisons of the membranes were performed with respect to the same projection area. The surface roughness parameters between the methanol solution- and isopropanol solution-treated samples are found to be different. For the aqueous methanol-treated membrane samples ME50 and ME99, the peak-to-peak distance (S_y) and the mean peak (μ) are respectively ~ 1 and ~ 0.5 μm in 5 × 5 μm^2 image size and ~ 1.7 and ~ 0.8 μm in 20 × 20 μm^2 image size. In case of aqueous isopropanol-treated membrane samples IPA50 and IPA99, these S_y and μ values are found to be slightly larger which are measured as ~ 1.1 and ~ 0.5 μm in 5 × 5 μm^2 image size and ~ 2 and ~ 0.8 μm in 20 × 20 μm^2 image size. For the neat sample, the S_y and μ values are decreased by about 50%. Similarly, the average arithmetic roughness (S_a) and the root mean square roughness (S_q) values for the neat sample are found to be the least which are measured as 0.064–0.124 μm and 0.081–0.157 μm, respectively. The S_a and the S_q values are the highest in case of isopropanol solution-treated samples which is about three times of the values for the neat sample. This may be related to strong absorption of isopropanol in the membrane film which subsequently distorts the surface morphology of the membrane.

Figure 10 shows the SEM images of the membrane surfaces of the NEAT, ME99, and IPA99 samples. The nodular hill-valley morphology typical of reverse osmosis polyamide membrane is again clearly evident in the SEM image of NEAT sample. The ME99 and IPA99 surfaces show different microstructural morphologies than the original morphology of reverse osmosis polyamide membrane. The fine nanoscale textures of the original hill-valley morphology had been damaged on the treatment of membranes with methanol or isopropanol solutions. Microscale-rugged surface morphologies were observed in the alcohol-treated samples. The changes in the surface morphologies observed by the SEM study are in agreement with the AFM results. The performances of the membranes after the alcohol treatments were different from the original performance of the neat membrane. Originally, the neat membrane exhibit permeate flux of about 60 L m^{-2} h^{-1} and S/R (salt rejection efficiency) selectivity of about 97% when tested on a batch type RO test kit under a standard testing condition with NaCl solution of 2000 ppm concentration at operating pressure of 250 psi. There were increases in permeate fluxes of the alcohol-treated membranes even though there was a slight decrease in selectivity (salt rejection efficiency). The flux enhancement was relatively more in case of the isopropanol-treated sample than the methanol-treated sample which may be related with the extent of changes observed on the membrane surfaces as for the reason that there was a large absorption of isopropanol in the polymer structure; however, in case of aqueous methanol solution-treated samples, the strong interaction

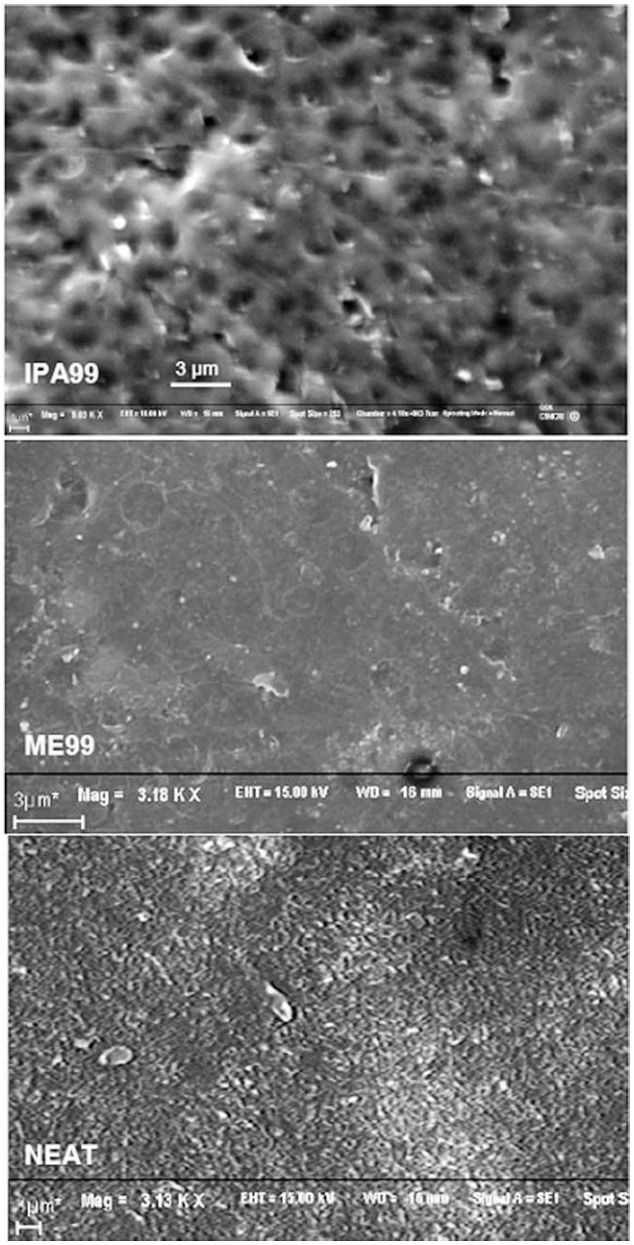

Figure 10 SEM images of the membrane surfaces of the neat and the alcohol solution-treated samples.

between the polyamide functional group and alcohol was not observed even though there was a change in surface roughness.

CONCLUSIONS

The ATR-IR technique provides necessary information for studying water and alcohol sorption on the membranes. The peak at 1640 and 2840–2970 cm^{-1} corresponding of water bending mode and aliphatic stretching vibrations were used to investigate the water and alcohol sorption, respectively, in the membrane. Preferential sorption of water over alcohol was observed in the membrane. However, it was found that the small amount of alcohol present in the polyamide layer resulted to the change of the original surface roughness of 0.060–0.120 μm range to 0.180–0.350 μm range which corroborates with the change in the absorbance peak intensities of polyamide. The results further demonstrated that the amount of alcohol absorbed by the polyamide layer of reverse osmosis membrane was related to the degree of changes in surface morphology of the surface polyamide layer. Therefore, the result presented shows a better understanding on the stability of the membrane in aqueous alcohol solution which is important to understand on how to improve the membrane for the long-term stability and performance in aqueous media containing organics.

The authors thank J. Chaudhuri for assistance in SEM study of the samples.

References

1. Cadotte, J. E. US Patent 1981,4,277,344.
2. Wang, H.; Li, D. J Mater Chem 2010, 20, 4551.
3. Greenlee, L. F.; Lawler, D. F.; Freeman, B. D.; Marrot, B.; Moulin, P.; Water Res a journal of the International Water Association 2009, 43, 2317.
4. Baker, R. W. Membrane Technology and Applications, 2nd ed.; Wiley, 2004.
5. ASM International®, Characterization and failure analysis of plastics, ASM International, Materials Park, Ohio, USA, 2003.
6. Mukherjee, D.; Kulkarni, A.; Gill, W. N. Desalination 1996, 104, 239.
7. Cai, B.-X. J Appl Polym Sci 2004, 92, 1005.
8. Aharoni, S. M. J Appl Polym Sci 1992, 45, 813.
9. Grulke, E. A. In: Polymer Handbook, 3rd ed.; Brandrup, J.; Immergut, E. H., Eds.; Wiley: New York, 1989 pp. 519–559.
10. Kesting, R. E. Synthetic Polymeric Membranes: A Structural Perspective; Wiley, 1985; Chapter 5.
11. Nguyen, T. D.; Chan, K.; Matsuura, T.; Sourirajan, S. Ind Eng Chem Prod Res Dev 1984, 23, 501.
12. Sharma, R. R.; Agrawal, R.; Chellam, S. J Membr Sci 2003, 223, 69.
13. Sharma, R. R.; Chellam, S. Environ Sci Technol 2005, 39, 5022.
14. Sharma, V. K.; Singh, P. S.; Gautam, S.; Maheshwari, P.; Dutta, D.; Mukhopadhyay, R. J Membr Sci 2009, 326, 667.
15. Sharma, V. K.; Singh, P. S.; Gautam, S.; Mitra, S.; Mukhopadhyay, R. Chem Phys Lett 2009, 478, 50.
16. Singh, P. S.; Aswal, V. K. J Phys Chem C 2007, 111, 16219.
17. Jadav, G. L.; Singh, P. S. J Membr Sci 2009, 328, 257.
18. Singh, P. S.; Aswal, V. K. J Colloid Interface Sci 2008, 326, 176.
19. Singh, P. S.; Joshi, S. V.; Trivedi, J. J.; Devmurari, C. V.; Rao, A. P.; Ghosh, P. K. J Membr Sci 2006, 278, 19.
20. Belfer, S.; Gilron, J.; Kedem, O. Desalination 1999, 124, 175.
21. Rao, A. P.; Joshi, S. V.; Trivedi, J. J.; Devmurari, C. V.; Shah, V. J. J Membr Sci 2003, 211, 13.
22. Kwak, S.-Y.; Jung, S. G.; Yoon, Y. S. Environ Sci Technol 2001, 35, 4334.
23. Bowen, W. R.; Doneva, T. A.; Stoton, J. A. G. Colloid Surf A 2002, 201, 73.
24. Kwak, S.-Y.; Ihm, D. W. J Membr Sci 1999, 158, 143.
25. Teng, M.-Y.; Lee, K.-R.; Fan, S.-C.; Liaw, D.-J.; Huang, J.; Lai, J.-Y. J Membr Sci 2000, 164, 241.